Fractal dimension of the strange attractor of the bouncing ball circuit

B. K. Clark, R. F. Martin, Jr.,[a] R. J. Moore,[b] and K. E. Jesse
Department of Physics, Illinois State University, Normal, Illinois 61790-4560

(Received 17 December 1993; accepted 22 August 1994)

We address the problem of distinguishing regular, chaotic, and random behavior using an electronic circuit modeling of a ball bouncing on an oscillating table. We calculate the correlation dimension of the system from time series data taken from the circuit, and show that this system seems amenable to correlation dimension analysis. In particular we find dimensions of 1.07 for regular data and 1.7 for chaotic data, while random data give no finite dimension. We conclude that the system apparently has a chaotic attractor of low dimension. The experiment and data analysis make a useful module to introduce advanced undergraduate students to nonlinear systems. © *1995 American Association of Physics Teachers.*

I. INTRODUCTION

In the last few decades nonlinear physical systems have become a major object of research in physics and other sciences. New techniques, many of them computational, have been developed to study nonlinear systems. An important goal for physics education is to introduce physics majors to this exciting new field and the new techniques developed for analyzing such systems. With this idea in mind, we have begun development of instructional modules for upper division physics courses dealing with nonlinear systems. This effort is closely associated with our department's evolving effort to integrate computational techniques into the physics major curriculum.[1] In this paper we present a model in which students investigate a nonlinear circuit. They analyze the data with elementary techniques of time series analysis and nonlinear dynamics.

Our main goals in developing this project are to provide a simple, real-world system for students to study as an experiment and to analyze with standard computational methods. In particular, we would like students to be able to discriminate between deterministic chaotic motion, regular motion, and nondeterministic noise. The system we chose is basically the circuit developed by Zimmermann *et al.*[2] to simulate a ball bouncing on an oscillating table. The circuit can be described using the dynamical variables position and velocity and a time-dependent force. It is readily constructed from standard elements, and it is not difficult for students to understand. Students measure the position and velocity of the simulated ball as functions of time. The data are digitized and recorded with a computer based on an Intel 80386-SX microprocessor and equipped with an analog to digital converter.

Discrete samplings of the time series representing the positions, $x(t)$, and velocities, $v(t)$, of the ball are recorded. The time series are analyzed with several different methods, that include visual inspection of $x(t)$ and $v(t)$, phase portraits, Fourier analysis, and the computation of correlation dimensions. As shown by Zimmermann *et al.*[2] the system exhibits regular (periodic and quasiperiodic) behavior and chaotic behavior, depending on the values of the circuit parameters. Often visual inspection appears to discriminate between the two classes of motion. Further discrimination between regular and chaotic motion can be obtained by plotting the phase portrait [$x(t)$ vs $v(t)$] of a trajectory (also called an orbit) in its position-velocity phase space. Using these methods we have produced parameter space "maps" showing what types of apparent behavior to expect for a wide range of parameter values.

The eye can sometimes be fooled in distinguishing between regular motion with multiple frequency components (multiple periodic) and chaotic motion, so further discrimination is needed. We used the power spectrum for the next level of discrimination. The power spectrum of the time series representing periodic motion should show discrete frequencies, while chaotic motion should have continuous bands of frequencies. Simple numerical techniques are employed to compute the power spectrum with fast Fourier transforms. The power spectrum alone is still not a sufficient discriminator, since multiple periodic data can emulate continuous bands, for example. Moreover, noise also has a continuous frequency distribution, so we need a method to discriminate deterministic chaos from noise as well as from regular motion.

One technique used to distinguish between regular motion, chaotic motion, and nondeterministic noise in a time series of data representing a trajectory is to determine the correlation dimension of the physical attractor underlying the time series. Physical systems are classified into Hamiltonian systems and dissipative systems in the nonlinear dynamics literature. Hamiltonian systems are governed by Hamilton's equations without dissipation, while dissipative systems involve physical dissipative mechanisms such as friction, viscosity, and electrical resistance. Dissipative systems are characterized by "attractors" that are subsets of the system's phase space into which orbits are attracted asymptotically in time. Attractors can be periodic and regular or chaotic (often called "strange attractors"). Regular attractors form subsets of integer dimension in the full phase space, while chaotic attractors typically have noninteger, or fractal dimensions. We have used the numerical technique of Grassberger and Procaccia[3] (these articles will be referred to as GP throughout this paper) for computing the dimension of an attractor. Bergé *et al.*[4] and Hilborn[5] also have excellent discussions of the technique. Application of this method to real experimental data is still somewhat controversial, and one of our goals is to see how well this technique works for our system. We show in Sec. III that the method does appear to distinguish between the three types of behavior. We discuss some subtleties in interpreting the results in Sec. IV.

The instructional module presented here serves several purposes. First, it is a practical introduction to nonlinear dynamics and chaotic behavior, helping students to begin developing their intuition regarding such systems. Second, the students are introduced to experimental techniques in data acquisition and computational techniques of data analysis, including the calculation of the power spectrum and correlation dimension. These techniques are currently used for data

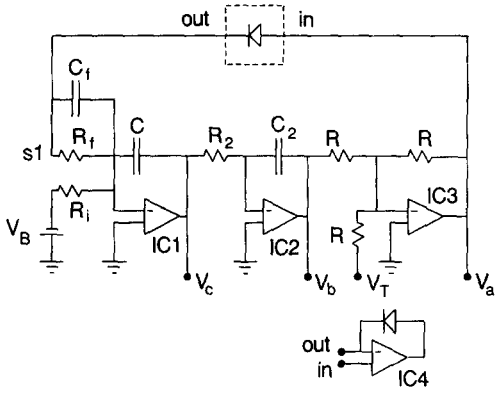

Fig. 1. Circuit diagram for bouncing ball circuit. R_2 and all R and 10 kΩ. R_f is a 1 kΩ resistor in series with a 2.5 kΩ potentiometer. R_i is a 1 MΩ resistor. C_f, C_2, and C are 0.05 μF. The rectifier in the dashed box is a precision rectifier based on IC4 as shown at the bottom of the figure. Each integrated circuit is an LF356. Note that C_f, C, R_f, R_i and the negative input of IC1 all have a common point of contact.

analysis in many branches of science and engineering. This module is suitable for use in a variety of courses, including an advanced laboratory, an electronic circuits course, and a course in nonlinear science.

The experimental setup, basic measurements, and qualitative descriptions of the circuit behavior are described in Sec. II. The quantitative data analysis methods and results are presented in Sec. III, and discussion and conclusions are included in Sec. IV.

II. THE EXPERIMENT

In the past 20 years the chaotic dynamic properties of the bouncing ball have been of great interest.[6–11] The electronic circuit that we used to simulate a ball bouncing on a moving table is basically the same as the one described by Zimmermann *et al.*[2] The circuit diagram is shown in Fig. 1. Our analysis of the circuit is somewhat different than their analysis. The core of this circuit consists of three LF356 JFET operational amplifiers. IC1 and IC2 are operational amplifiers connected as integrators in series followed by an operational amplifier, IC3, used as a unity gain adder. The output of the adder is fed back to the first integrator through IC4, that is used as a precision rectifier.

Zimmermann *et al.*[2] have established that $-V_T$ is analogous to the oscillating table position on which the mechanical ball bounces. V_T serves as the driving force for a forced damped harmonic oscillator, and it is a sine wave provided by a function generator. They also showed that V_b is analogous to the position of the ball above the zero displacement position of the table. IC2 integrates the input, V_c, which is proportional to the velocity of the ball. The actual velocity is $-V_c/(R_2C_2)$. The output of IC3 is the inverted sum of V_T and V_b. When V_a is positive, the precision diode conducts and the voltage at $s1$ is equal to V_a, so

$$V_{s1}=V_a=-V_b-V_T=[1/(R_2C_2)]\int V_c dt-V_T. \quad (1)$$

The phase inversion causes the voltage at V_c to represent the negative of the ball velocity. Consequently, V_b represents the position of the ball.

The relationship between the input and output voltages of IC1 can be written as

$$V_{s1}/R_f+C_f dV_{s1}/dt-V_B/R_i=-C dV_c/dt. \quad (2)$$

R_f in our circuit is a 1 kΩ resistor in series with a 2.5 kΩ variable resistor. The value of R_f is analogous to the coefficient of restitution of the ball, which we can vary. V_B is a 1.4 V battery, which simulates part of a constant acceleration. When Eq. (1) and its derivative are submitted into Eq. (2), with $V_{s1}=V_a$, one obtains

$$dV_c/dt+V_c/\tau+\omega_0^2\int V_c dt$$
$$=V_T/(R_fC)+(C_f/C)dV_T/dt+V_B/(R_iC), \quad (3)$$

where $\tau=R_2C_2C/C_f$ and $\omega_0=(1/\tau R_fC_f)^{1/2}$. This is Eq. (12) in Zimmermann *et al.*[2] but they neglected a C in the first two terms on the right-hand side of the equation. As they state, this equation is that of a forced damped harmonic oscillator subject to a constant force and two time-dependent forces. The constant force comes from the term involving V_B, and the time-dependent forces are from the terms with V_T and dV_T/dt. As written in Eq. (3) each of the three terms on the right-hand side are analogous to accelerations. The nonconducting state of the precision diode circuit results when V_a goes negative. The effect of this condition in the circuit can be understood by allowing $R_f\to\infty$ and $C_f\to 0$ in Eq. (3). Here, the acceleration terms involving V_T, dV_T/dt, V_c/τ, and ω_0^2 all vanish. Equation (3) reduces to

$$dV_c/dt=V_B/(R_iC). \quad (4)$$

This equation describes uniformly accelerated motion in which $V_B/(R_iC)$ is the analog of the constant acceleration due to gravity to which the ball is subject in free fall. When V_a is positive, Eq. (3) describes the acceleration forces on the ball when it is in contact with the table.

V_b and V_c are connected to the inputs of an analog to digital converter that converts each value approximately 1000 times per second. The converted values are recorded with an Intel 80386-SX based personal computer. The results can then be analyzed on the personal computer or transported to a workstation for analysis. An oscilloscope is also used to monitor V_b and V_c.

This circuit can exhibit periodic, chaotic, and a borderline periodic–chaotic behavior. Figure 2 shows segments of time series of data for a periodic case and a chaotic case. Although the eye can easily detect a difference between these plots, a phase space plot of $x(t)$ vs $v(t)$ (a "phase portrait") shows the characteristics of the motion more clearly, as can be seen from Fig. 3. These phase portraits are equivalent to what is observable on the oscilloscope by plotting the ball velocity on the vertical axis and the ball position on the horizontal axis. The trajectory of the regular orbit [Fig. 3(a)] is not a well-defined narrow curve as might be expected, but there is broadening of the periodic orbit due to noise inherent in the experimental setup. One component of noise comes from the circuit itself, and another component is caused by fluctuations in the driving frequency. The chaotic orbit shown in Fig. 3(b) clearly represents more complex dynamics than is depicted in Fig. 3(a), but the finite width of the periodic orbit will not always allow visual discrimination of orbit types.

Nevertheless, we used visual discrimination as a first pass at organizing the data. The frequency and amplitude of V_T were systematically varied for each selected value of R_f. The

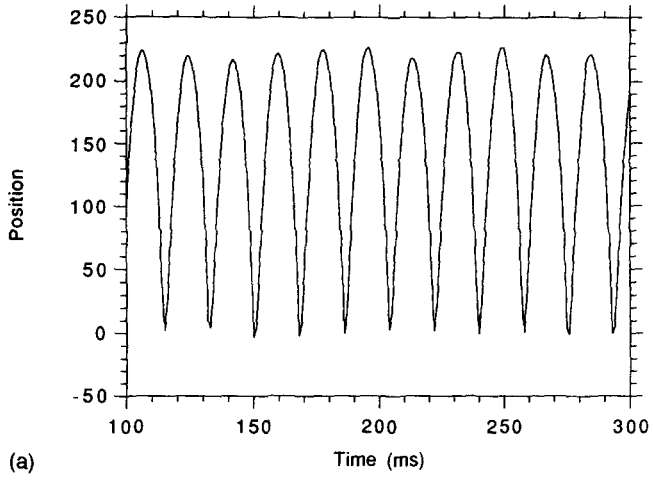

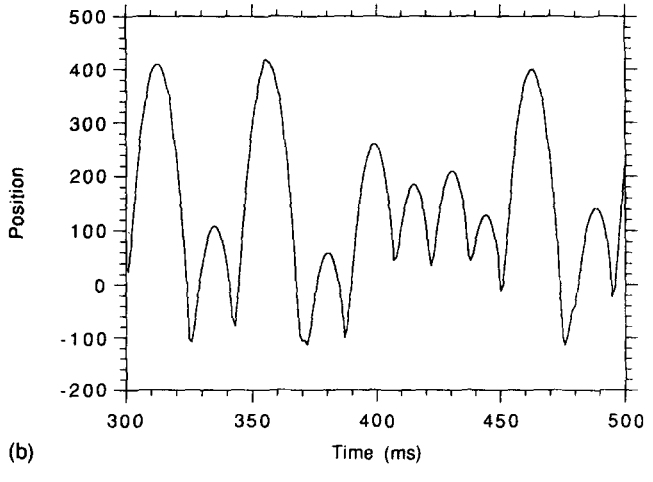

Fig. 2. Segments of position time series obtained for regular and chaotic time series. A segment of a regular time series is shown in (a) where the table frequency was 55 Hz, the table amplitude was 0.85 V, and the value of R_f was 1500 Ω. A segment of a chaotic time series is shown in (b) where the table frequency was 66 Hz, the table amplitude was 1.25 V, and the value of R_f was 1500 Ω.

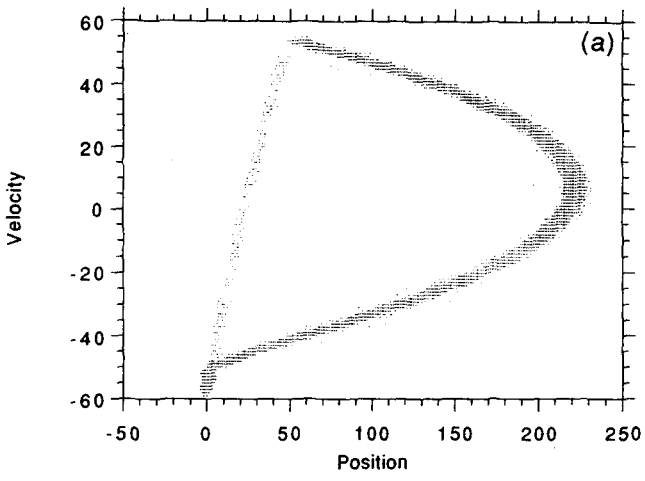

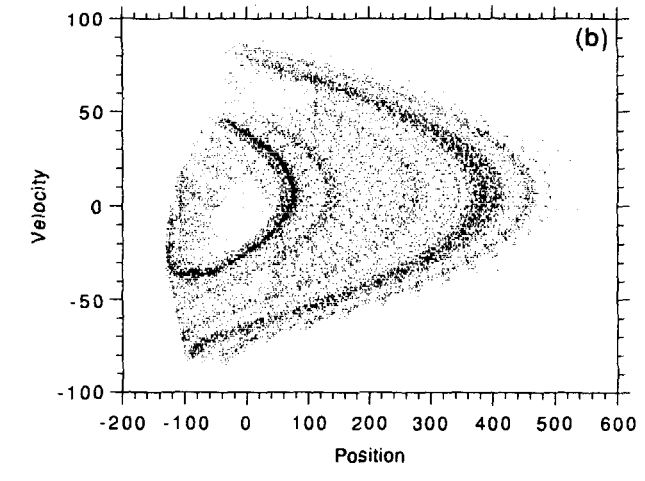

Fig. 3. Phase space plots of velocity vs position for (a) the regular time series and (b) the chaotic time series. The parameters are the same for this plot as for Fig. 2.

resultant circuit behavior was classified as periodic, chaotic, or borderline based on the phase space portrait displayed on the oscilloscope as described by Zimmermann *et al.*[2] The results are shown in Fig. 4. Figure 4(a) shows the map obtained for R_f=1095 Ω. There is a clear distinction between periodic regions and apparent chaotic regions as the frequency of V_T is varied at small amplitudes. The regions are compressed and intertwined at larger values of V_T. The chaotic behavior begins at lower frequencies as the amplitude is increased. When the value of R_f was increased to 1500 Ω [Fig. 4(b)] the regions of chaotic and periodic behavior became more intertwined. The regions were intertwined over a large frequency range at low amplitude at R_f=1800 and 2500 Ω [Figs. 4(c) and 4(d)]. R_f=1500 Ω provided reasonably distinct regions to quantify the differences in behavior between the chaotic and periodic regions.

III. DATA ANALYSIS

A second step in determining whether the position and velocity trajectories are periodic or chaotic is to calculate the power spectrum. The power spectrum for periodic, random (from a random number generator), and chaotic time series were calculated using the fast Fourier transform algorithm in Press *et al.*[12] on an IBM RS/6000. The results are shown in Fig. 5. The periodic time series [Fig. 5(a)] shows a sequence of peaks at 55, 110, 165, 220, 275, 330, 385, and 440 Hz. The frequency of V_T is 55 Hz. A second set of peaks is present to the low frequency side of many of the harmonics, but they are several orders of magnitude weaker. We do not understand the source of this set of peaks, but clearly their separation is nearly the same as for the first set of peaks.

The power spectrum of the chaotic time series [Fig. 5(b)] shows less structure. The peak at 66 Hz corresponds to the driving frequency of V_T, and harmonics at 132 and 198 Hz are weakly visible. There appear to be two broad maxima near 22 and 42 Hz (possibly subharmonics) and another maximum near 110 Hz that is several orders of magnitude weaker, but the exact origin of these maxima is unclear. Thus, while the spectrum shows some continuous bands, it also has some regular structure, implying that this is not a decisive method to distinguish chaos from regular motion.

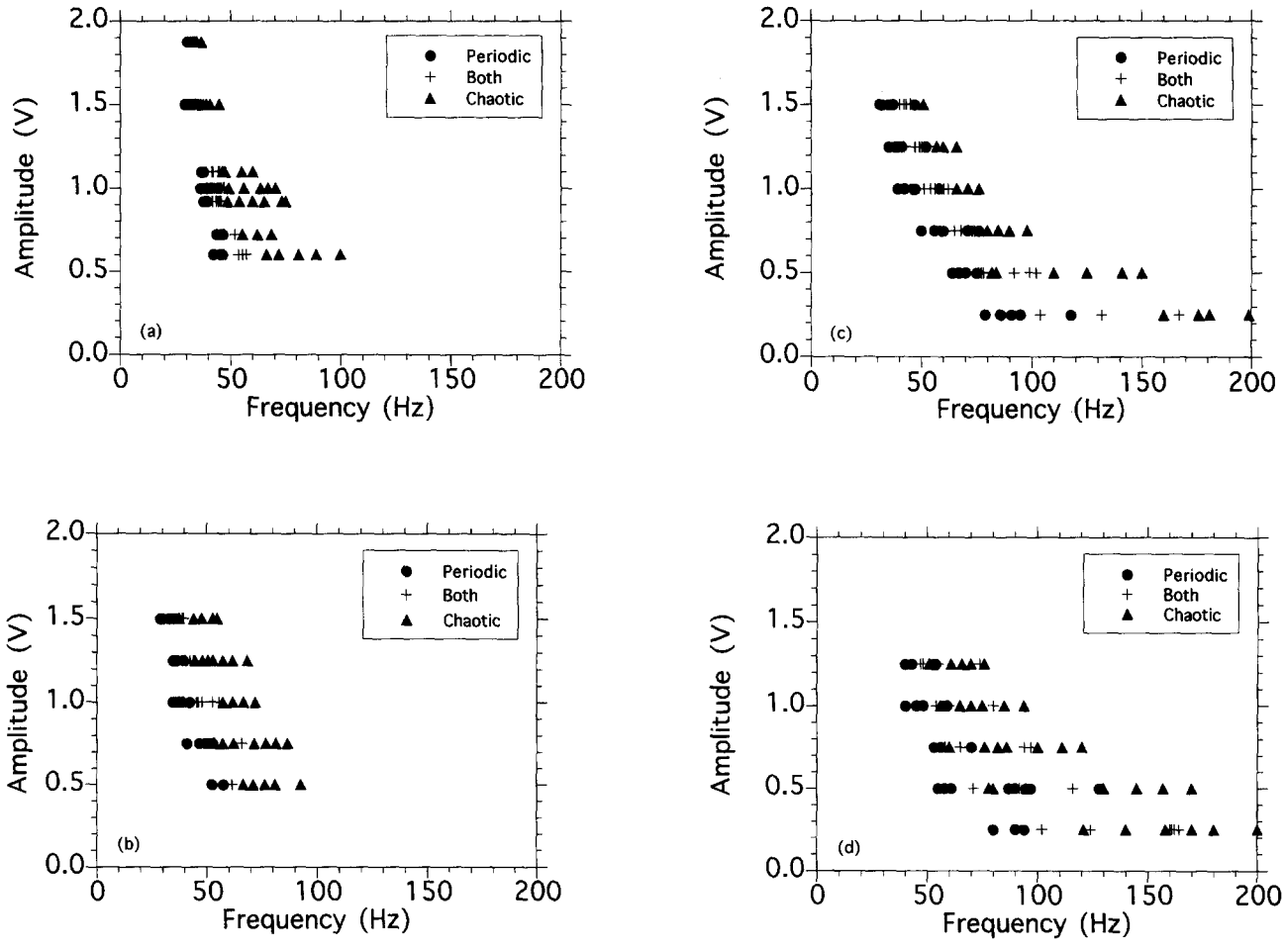

Fig. 4. Parameter maps showing regions of periodic behavior, chaotic behavior, and both. R_f was 1095 Ω in (a), 1500 Ω in (b), 1800 Ω in (c), and 2500 Ω in (d). In each case, an oscilloscope is operated with its channel 1 as the x axis and its channel 2 as the y axis. V_c is connected to channel 1 and V_b is connected to channel 2. The resulting patterns for each combination of frequency, table amplitude, and value of R_f are similar to those shown in Fig. 3, but rotated 90°. Each pattern is classified as periodic if it is similar to Fig. 3(a), chaotic if it is similar to Fig. 3(b), and both if it displays elements of both Figs. 3(a) and 3(b).

To go beyond power spectral analysis, the correlation dimensions of the chaotic and periodic trajectories can be calculated according to the methods of GP. The basic idea is as follows (excellent discussions in more depth can be found in Refs. 4 and 5): one imagines embedding the attractor, as exemplified by the experimental orbit, in a space of dimension, n. We then ask the question: how does the number of points, $N(r)$, enclosed in a sphere of dimension, n, depend on the radius, r, of the sphere? In general, one expects $N(r)\sim r^{\nu}$; e.g., if the orbit is a simple curve $\nu=1$, no matter what the dimension of the sphere. Similarly, if the attractor is uniformly distributed on a plane, $\nu=2$ for sphere dimensions greater than 2. Alternatively, ν should increase linearly as n increases for random noise with an infinite number of degrees of freedom, without reaching a limiting value. Deterministic chaos will have a finite but noninteger value for ν, i.e., ν should reach a noninteger limit as the embedding dimension n increases. This limit gives the (fractal) dimension of the attractor.

The first step in calculating the correlation dimension with a single time series is to "reconstruct" the phase space in the embedding dimension, n, i.e., map the time series of points into N vectors of dimension, n, according to

$$\mathbf{X}_i=\{x(t_i),x(t_i+T),\ \ldots,x[t_i+(n-1)T]\}, \tag{5}$$

where T is the delay time between components. In practice T is just an integer spacing between components (e.g., $\mathbf{X}_1=\{x_1,x_5,x_9\}$ is a valid vector in three-dimensional space). Additional vectors are similarly picked (e.g., $\mathbf{X}_2=\{x_2,x_6,x_{10}\}$ and so on). Once all of the vectors for a given dimension have been established, one defines the correlation integral sum as

$$C(N,r)=(2/N^2)\sum_{i=1}^{N-5}\sum_{j=i+5}^{N}\Theta(r-|\mathbf{X}_i-\mathbf{X}_j|), \tag{6}$$

where Θ is the step function, i.e., $\Theta(y)=1$ if $y>0$ and $\Theta(y)=0$ otherwise. Note that the summation essentially counts the number of points within a sphere of radius r. Hence, if $C(N,r)$ is calculated for a range of r and the slope of $\log C(N,r)$ vs $\log r$ is plotted against n, then the correlation dimension is the value of the slope of this plot when it reaches a plateau. Embedding dimensions up to at least $2D+1$ should be used to obtain a reliable correlation dimension of D.[13] Again, this is not a strong limitation for our data sets.

Although this circuit allows easy measurement of the two relevant dynamical variables, this is not generally true in more complex systems. Often one has data from one physi-

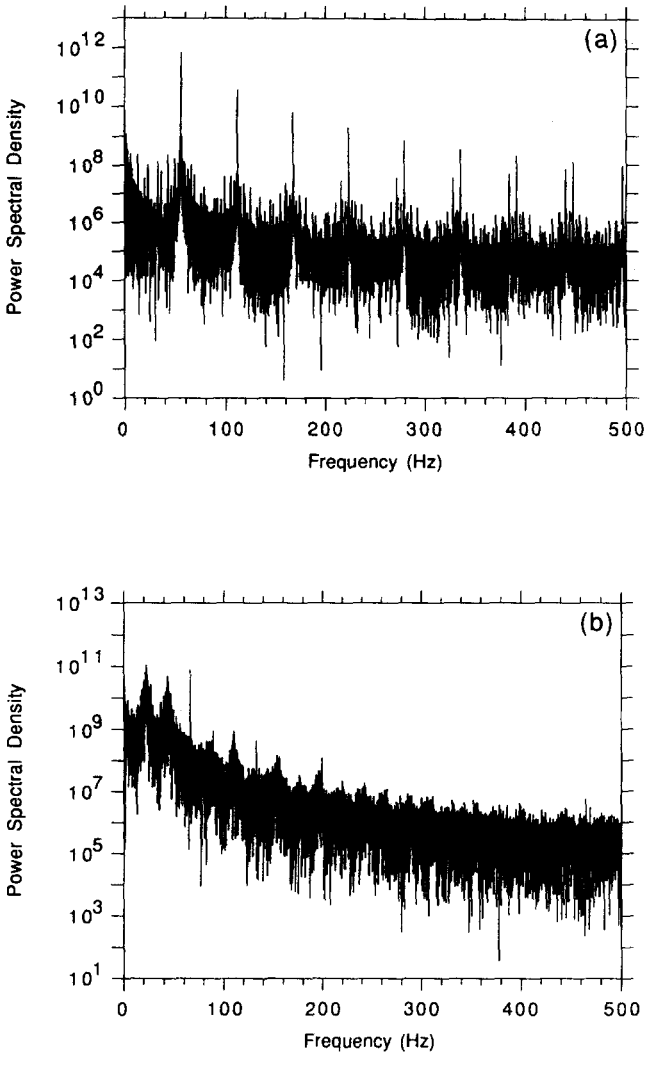

Fig. 5. Power spectrum of the same periodic and chaotic time series shown in Figs. 2 and 3. The power spectrum for the periodic series is shown in (a) and the power spectrum for the chaotic series is shown in (b).

cal property of a system which may have many dynamical variables (or an infinite number as in continuous systems). Thus, we prefer to apply the GP method to only one time series, the position data, rather than computing the correlation dimension directly from the two time series. To obtain a dimension, D, for a strange attractor one needs at least $10^{D/2}$ data points in the time series.[14] With this circuit it is easy to obtain long time series, so treating the position series alone is not a great restriction. For example, with 15 000 points from a position time series (recorded at a rate of approximately 1 kHz for all time series and a driving frequency of 55 Hz for the chaotic time series) we can reliably study a chaotic attractor with a dimension of no more than $D=8$. This is sufficient for our purposes.

Figure 6(a) shows plots of the value of $\log C(N,r)$ vs $\log r$ for embedding dimensions 1–7, from upper left to lower right, for 15 000 vectors from the chaotic time series. The correlation dimension for each curve is obtained as the slope of the linear portion of the curve. These linear segments as well as their calculated slopes are shown in Fig. 6(b) for the chaotic data. The slopes begin at 0.96 for an embedding dimension of 1, increase to 1.7 for an embedding dimension of 4, and remain constant at about 1.7 as the embedding dimension is increased to 7. For periodic data, the slopes quickly reach a constant value of 1.07, as shown in Fig. 6(c). Finally, the slopes for the nondeterministic noise continue to increase as the embedding dimension is increased. This is shown in Fig. 6(d).

Figure 6(e) shows a summary plot of the slopes of the $\log C(N,r)$ vs $\log r$ plots for the periodic, chaotic, and nondeterministic noise as a function of embedding dimension. These are the results of Figs. 6(b)–6(d) in a format which highlights the plateau in the slopes shown by the periodic and chaotic time series. From this it appears that a clear distinction can be made between orbit types. That is, we expect the periodic orbit to have integer dimension 1.00, which is consistent with our value of 1.07. The small difference is attributable to noise, as will be discussed presently. The chaotic orbit yields a noninteger dimension 1.7, higher than the regular orbit but sharply different from random noise. The validity and utility of these results are discussed in the next section.

IV. DISCUSSION AND CONCLUSION

We saw in the last section that the bouncing ball circuit leads to time series that can be fruitfully analyzed. We observed a definite difference between orbits appearing regular and those appearing chaotic using each of several techniques: visual inspection, phase portraits, power spectra, and correlation dimension. We estimated a dimension of 1.07 for the periodic data and 1.7 for the chaotic series. It is tempting to conclude immediately that we have a definitive method for discrimination between regular and chaotic motion. However, as mentioned in Sec. I, care must be taken in interpreting these results.

First, not all the observations are as clean as those presented here. For this analysis we purposely chose parameter values where a reasonably clear distinction in orbit type could be made visually (see Sec. II). For high values of R_f and V_T small changes in resistance could change the orbit type, implying close spacing between chaotic and regular regions. Moreover, for some parameter values, time series ensued which appeared to change back and forth from regular to chaotic behavior in an unpredictable way. This behavior shows either that the circuit parameters are not perfectly stable, or that some source of noise is perturbing the system from one attracting region to another. For such cases, where the measurement itself is difficult, we expect the data analysis techniques to be less useful. For example, it is unclear how to interpret the correlation dimension of a time series that changes between periodic and chaotic motion.

There are also limitations to the data analysis techniques, even when applied to good data. The difficulty in distinguishing between multiple periodic, chaotic, and noisy signals with Fourier techniques is well known; indeed, that is why other methods have been developed. The difficulties of the GP method are less well understood. We have already mentioned the logarithmic dependence on number of data points in Sec. II, so as a minimum condition, one needs to be sure to obtain sufficient measurements to utilize the technique. Less well understood is the effect of the free parameter T in reconstructing the attractor for the calculation of the correlation dimension. It appears to be a bit of an art to choose a "suitable" value of T for a given set of data. For nonlinear maps such as Henon's map (see Bergé, *et al.*, Ref.

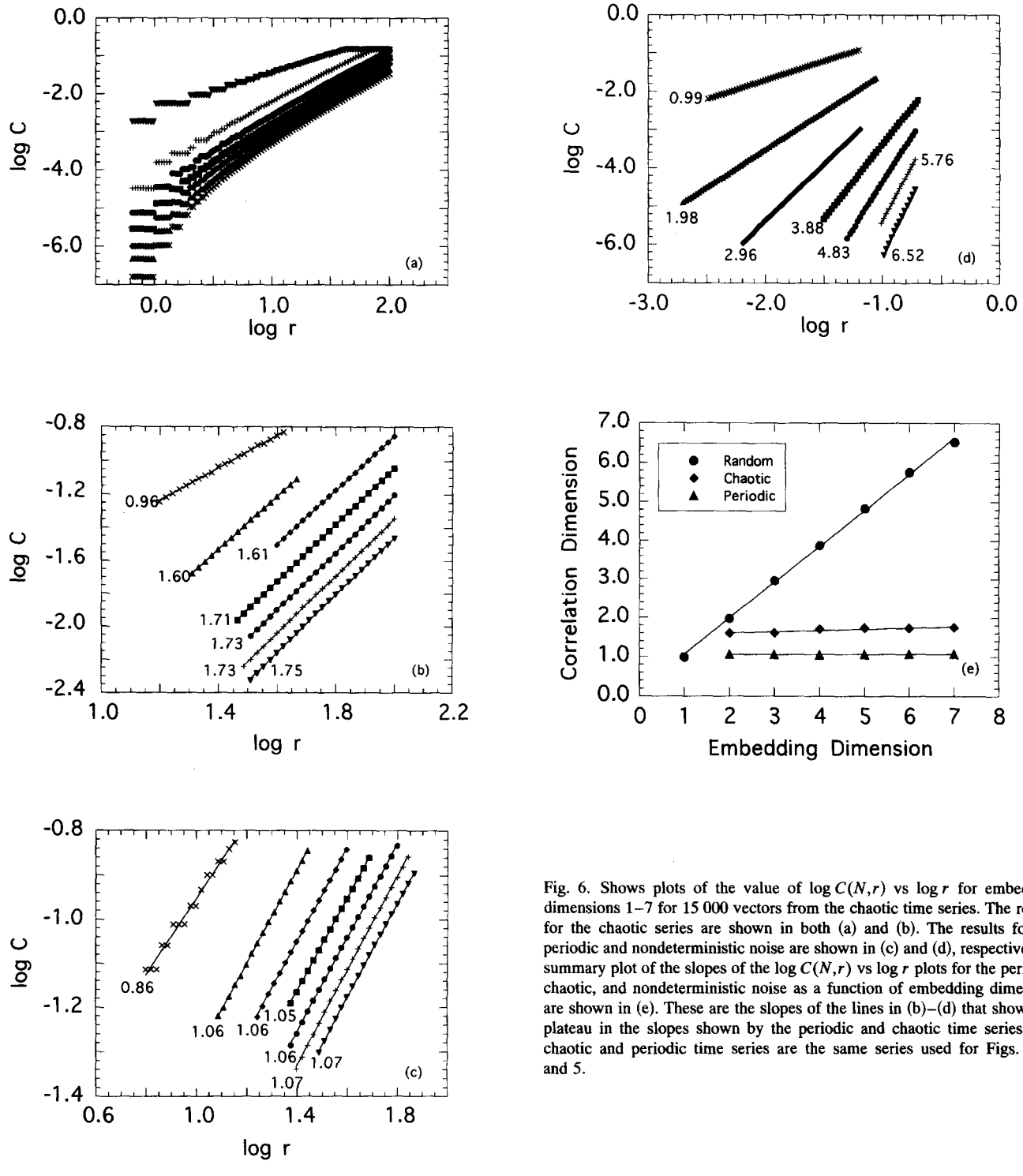

Fig. 6. Shows plots of the value of $\log C(N,r)$ vs $\log r$ for embedding dimensions 1–7 for 15 000 vectors from the chaotic time series. The results for the chaotic series are shown in both (a) and (b). The results for the periodic and nondeterministic noise are shown in (c) and (d), respectively. A summary plot of the slopes of the $\log C(N,r)$ vs $\log r$ plots for the periodic, chaotic, and nondeterministic noise as a function of embedding dimension are shown in (e). These are the slopes of the lines in (b)–(d) that shows the plateau in the slopes shown by the periodic and chaotic time series. The chaotic and periodic time series are the same series used for Figs. 2, 3, and 5.

15, for example) small values of T give the best correspondence between the actual attractor and the reconstructed attractor, while for real data one may need a larger value of T to avoid autocorrelation between the data points.[16] Liebert and Schuster[17] present a more systematic way of choosing T.

Since we are trying to distinguish between noise and deterministic chaos, noise caused by power supply fluctuations and the resolution of the analog to digital converter cause problems. In our circuit we found that noise smeared out the regular orbits somewhat in phase space. One expects that noise would cause the $\log C(N,r)$ in Fig. 6(b) to increase more with $\log r$ [viz. Fig. 6(d)] and turn over at an artificially high value, thus overestimating the correlation dimension. Our result of 1.07 for the regular orbit correlation dimension is consistent with this view (one would expect 1.00 for a true periodic orbit). Various techniques have been tried to deal with noise when applying the GP method, e.g., the singular spectrum analysis.[18] Suffice it to say there is no clear solution at this point.

A more subtle problem is the basic applicability of the method. It has been shown that certain types of colored noise[19] can result in finite correlation dimensions (i.e., they can emulate deterministic chaos), unlike our noise result in

Fig. 6(d). Also, systems with long autocorrelation times give spurious results with the GP algorithm.[20] Thus, the results of GP analysis must (for this and other reasons) remain nondefinitive. Other techniques, typically more involved, have been developed to assist in the discrimination between regular and chaotic motion, a well-known one being the computation of the Lyapunov exponents.[21] Other methods are currently being developed.[22]

Our results indicate that the GP method may work well with the bouncing ball circuit, in the parameter regime studied. In particular, for application in an advanced undergraduate course, we feel the results are good enough to introduce students to the experimental study of nonlinear systems (with all its pitfalls!). Interested students could probe further using Lyapunov exponent or noise-reduction techniques.

Finally, it is worth mentioning why the correlation dimension is useful for strange attractors. If one can convincingly show that the system has a strange attractor, then the correlation dimension, D, represents the minimum number of variables necessary to describe the attractor. More precisely, the number of degrees of freedom needed to describe the system is between D and $2D+1$.[13] The technique is most useful for more complex systems that require many dynamical variables or have no good theoretical description at all. Then, from a single experimental time series, one can hope to determine whether the behavior of the attractor can be described with only a few variables. Thus, in some sense, systems with low dimensionality are simple systems even though they exhibit seemingly complex behavior. Determination of the relevant independent variables is nontrivial, although mathematical methods of finding basis variables and building model systems based on them have been developed.[23] Our circuit is a simple system to begin with, requiring two dynamical variables (V_c and V_b, or the ball velocity and position, respectively) and a time-dependent force, equivalent to three variables with no explicit time dependence. Our correlation dimension of 1.7 for the chaotic orbit presented in Sec. III would imply that at least two independent variables are required to describe the attractor in this parameter regime, fewer than the actual dynamical dimension of 3.

ACKNOWLEDGMENTS

We gratefully acknowledge fruitful discussions with H. Matsuoka and the assistance of M. Ruesink with data taking. R.F.M. appreciates the hospitality of CRPE and recognizes the partial support of NSF Grant No. DUE 9352362.

[a]Currently on leave at Centre de Recherches en Physique de l'Environment (CRPE), Saint-Maur des Fossés, France.

[b]Current address: Department of Atmospheric Sciences, University of Illinois at Urbana–Champaign, Urbana, IL.

[1]Richard F. Martin, Jr., George Skadron, and Robert D. Young, "Computers, physics and the undergraduate experience," Comput. Phys. **5**, 302–310 (1991).

[2]Robert L. Zimmermann, Sergio Celaschi, and Louis G. Neto, "The electronic bouncing ball," Am. J. Phys. **60**, 370–375 (1992).

[3]Peter Grassberger and Itamar Procaccia, "Measuring the strangeness of strange attractors," Physica D **9**, 189–208 (1983); Peter Grassberger and Itamar Procaccia, "Characterization of strange attractors," Phys. Rev. Lett. **50**, 346–349 (1983).

[4]P. Bergé, Y. Pomeau, and C. Vidal, *Order Within Chaos; Towards a Deterministic Approach to Turbulence* (Wiley, New York, 1990), pp. 130–135.

[5]Robert C. Hilborn, *Chaos and Nonlinear Dynamics* (Oxford University Press, New York, 1994), pp. 407–436.

[6]A. B. Pippard, *The Physics of Vibrations* (Cambridge University Press, Cambridge, 1978), Vol. 1, pp. 271–275.

[7]P. J. Holmes, "The dynamics of repeated impacts with a sinusoidally vibrating table," J. Sound Vibrat. **84**, 173–189 (1982).

[8]N. B. Tufillaro and A. M. Albano, "Chaotic dynamics of a bouncing ball," Am. J. Phys. **54**, 939–944 (1986).

[9]T. M. Mello and N. B. Tufillaro, "Strange attractors of a bouncing ball," Am. J. Phys. **55**, 316–320 (1987).

[10]Sergio Celaschi and Robert L. Zimmermann, "Evolution of a two-parameter chaotic dynamics from universal attractors," Phys. Lett. A **120**, 447–451 (1987).

[11]Robert L. Zimmermann and Sergio Celaschi, "Comment on Chaotic dynamics of a bouncing ball," Am. J. Phys. **56**, 1147–1148 (1988).

[12]William H. Press, Brian P. Flannery, Saul A. Teukolsky, and William T. Vetterling, *Numerical Recipes: The Art of Scientific Computing*, 1st ed. (Cambridge University Press, New York, 1986), pp. 381–407.

[13]F. Takens, "Detecting strange attractors in turbulence," in *Proceedings of the Symposium on Dynamical Systems and Turbulence*, University of Warwick, 1979–1980, edited by D. A. Rand and L. S. Young (Springer, Berlin, 1981), pp. 365–381.

[14]J.-P. Eckmann and D. Ruelle, "Fundamental limitations for estimating dimensions and Lyapunov exponents in dynamical systems," Physica D **56**, 185–187 (1992).

[15]Reference 4, pp. 144–154.

[16]S. Niel Rasband, *Chaotic Dynamics of Nonlinear Systems* (Wiley, New York, 1990), pp. 200–202.

[17]W. Liebert and H. G. Schuster, "Proper choice of the time delay for the analysis of chaotic time series," Phys. Lett. A **142**, 107–111 (1989).

[18]For a case in point see A. S. Sharma, D. Vassiliadis, and K. Papadopoulos, "Reconstruction of low-dimensional magnetospheric dynamics by singular spectrum analysis," Geophys. Res. Lett. **20**, 335–338 (1993).

[19]A. R. Osborne and A. Provenzale, "Finite correlation dimension for stochastic systems with power-law spectra," Physica D **35**, 357–381 (1989).

[20]James Theiler, "Spurious dimension from correlation algorithms applied to limited time-series data," Phys. Rev. A **34**, 2427–2432 (1986).

[21]Alan Wolf, Jack B. Swift, Harry L. Swinney, and John A. Vastno, "Determining Lyapunov exponents from a time series," Physica D **16**, 285–317 (1985).

[22]See, e.g. George Sugihara and Robert M. May, "Nonlinear forecasting as a way of distinguishing chaos from measurement error in time series," Nature **344**, 734–741 (1990); Richard Wayland, David Bromley, Douglas Pickett, and Anthony Passamante, "Recognizing determinism in a time series," Phys. Rev. Lett. **70**, 580–582 (1993).

[23]J. P. Crutchfield and B. S. McNamara, "Equations of motion from a data series," Complex Systems **1**, 417–421 (1987).

TOO MUCH HAPPINESS?

People are frightened by the thought of getting too much information, which just shows we're not in the Information Age yet. Are you frightened by the thought of getting too much money? Too much happiness?

Arno Penzias, quoted by James Gleick, "The Telephone Transformed—Into Almost Everything," *The New York Times Magazine*, May 16, 1993, p. 29.